A Simulation-Based Probabilistic Risk Assessment of Electric Vehicles Control Strategies Accounting Renewable Energy Sources

ROBERTO ROCCHETTA[1] and EDOARDO PATELLI[2]

[1] *Institute of Risk and Uncertainty, University of Liverpool, L69 3GQ, Liverpool, United Kingdom.*
E-mail: robertor@liverpool.ac.uk
[2] *Institute of Risk and Uncertainty, University of Liverpool, L69 3GQ, Liverpool, United Kingdom.*
E-mail: edoardo.patelli@liverpool.ac.uk

Distributed power Generator systems (DGs) and Renewable Energy Sources (RES) are promising technologies, which have been proven to be beneficial for the grid in several ways, e.g. improve voltage profile, reduce pollutant emissions and decrease power losses. Although an increasing renewable energy penetration may be beneficial, power produced by those devices is affected by high uncertainty, therefore can reduce power supply reliability, system non-linearity, overall complexity and provide new challenges for the future grid. Possibility of control charge and discharge of the Electric Vehicles (EV) batteries, makes EVs an interesting technology, which may allow increment in renewable penetration and prove ancillary service to the customers. In the last years, several works have been focused on optimal Vehicle to Grid (V2G) and Grid to Vehicle (G2V) control states, with respect to different objectives and goals. Nevertheless, risk assessment frameworks to compare EVs control schemes seems in need of further investigations. In this paper, a framework for EVs control strategies risk assessment and comparison is presented. The framework allows to account uncertainties due to intrinsic randomness in the environmental conditions and operative states of the system. A contingency analysis is performed and line overload and cascading index are obtained. A study case, the modified IEEE 24 nodes reliability test system, have been used as test system for the framework. Risk analysis and contingency ranking have been performed for three different EVs control strategies. Results show that this framework can be effectively used as platform for EVs control strategies comparisons accounting uncertainties.

Keywords: Probabilistic Risk assessment & Contingency ranking & Distributed Renewable energy sources & Vehicle to grid & Electric Vehicles Control Strategy

1. Introduction

Power distribution grid have been historically developed to withdraw electric power form the transmission grid and distribute it to various end-user loads. In the last decades, the classical distribution grid has deeply changed, becoming an active player in the power production.

Proc. of the 13th International Probabilistic Workshop (IPW 2015)
Edited by Edoardo Patelli & Ioannis Kougioumtzoglou

ISBN: 978-981-09-7963-8 — doi: 10.3850/978-981-09-7963-8_088

Renewable sources and distributed generators, e.g. Wind Turbines(WT), Photovoltaic (PV) generators and EVs, are playing dominant role in this shift. The integration of RES in the power grid appears to be beneficial, however, random behaviour in terms of produced power provides several challenges. For example, robustly estimate power supply reliability may require accurate uncertainty quantification.

Power grid risk assessment aims at estimating both the probability (or frequency) of disturbances to system operation and their consequences for the network as shown by J. McCalley et al. (2004). Probabilistic risk assessment can effectively handle randomness in power system security analysis and has been successfully used to analyse power system integrating with renewable energy generation, see as example R. Mena et al. (2014).

Electric Vehicles appear to be interesting technology for the future grid sustainability. M. Yilmaz et al. (2012) remark that, statistically, vehicles are driven only 4-5 % of the time, which makes the unexploited EVs battery capacities interesting for the power network aims. If adequately controlled, high EVs penetration can prove beneficial, e.g. M. van der Kam et al. (2015) shown increment in the renewable energy penetration, load demand peaks shaving and increased energy self-consumption. Nevertheless, limitations due to battery degradation, see L. Liu (2015), challenging communications between vehicles and grid and random EVs operative state are problematic aspects which demand for further analysis.

In the literature, works have focused on different EV control strategies, interaction with RES and power grid. Liansheng Liu et al. (2015) recently revised the interaction effect between RES and EVs within the smart grid. Kavousi-Fard et al. (2014) investigate optimal RES and EVs operational management by evolutionary-based optimization algorithm. In the micro-grid context, A. Kavousi-Fard et al. (2014) analysed the impact of different control strategies on battery life-time, micro-grid self-consumption and relative peak reduction with respect to a no-control reference scenario. In the work proposed by Z. Liu et al. (2014) and similarly H. Hashemi-Dezaki et al. (2015) reliability assessment frameworks for EV analysis focus on different reliability indexes.

Considered the works reviewed, it seems that a framework to vehicle to grid (V2G) and grid to vehicle (G2V) control strategies, with respect to contingency-induced overload and cascading risks, has not been fully investigated and requires further study. In this paper, main contribution is the development of a simulation-based probabilistic risk assessment framework which allows to include effect of RES uncertainty and analyses and compares risks of multiple EV control strategies. The framework allows comparison of the strategies with respect to grid risk.

2. Sequential Time Risk Assessment framework

Generally speaking, risk is often defined as the product of probability of occurrence of an undesired event (i.e. contingency) and the related consequence (i.e. severity).

As stated by Čepin (2005), a contingency in power system risk analysis can be defined as the unexpected loss of one element in the system (e.g. distribution line, transformer, generator, etc.). In line with works proposed by Rocchetta et al. (2015) and F. Xiao et al. (2009), but with different prospective, feeder over-load has been accounted as indicator of the system stress and post-contingency severity (because related with the feeder thermal limit and system stress). The risk index associated with a predefined set of contingencies and for the whole power network can be expressed as follows:

$$R(\zeta) = \sum_{i=1}^{N_C} R(C_i|\zeta) = \sum_{i=1}^{N_C} \sum_{k=1}^{N_l} \mathcal{P}(C_i|\zeta) SevOL_k(C_i, \zeta) \tag{1}$$

where ζ is the set containing all the considered operational and environmental information (e.g. wind speed, solar irradiation, load power demand, EVs operational state, simulated hour of the day, etc.), C_i is the i^{th} contingency listed, $SevOL_k(C_i, \zeta)$ is the overload severity for the line k after failure C_i occurred and under the condition ζ, N_l is the total number of lines in the system and N_c is the total number of contingencies listed. The composite risk index under the environmental-operational condition ζ is named $R(\zeta)$.

2.1. *Line Failure Probability*

The probability of each contingency takes into account the failure of a distribution line by a Poison distribution function as in J. McCalley et al. (2003):

$$\mathcal{P}(C_k) = (1 - \exp(\lambda_k l_k)) \exp(-\sum_{j \neq i} \lambda_j l_j) \tag{2}$$

where $\mathcal{P}(C_k)$ is the probability of line contingency k in the next 1 h, λ_k is the failure rate of the distribution line k per unit time and length and l_k source is the length of the i^{th} line.

2.2. *Overload Severity Functions*

Severity functions are used to quantify the extent of the failure, several type of severity exist in literature. The continuous severity function for overload is specifically defined for each circuit and it measures the extent of violation in terms of excessive power flow as the percentage of rating (PR_k), ratio between active power flowing in the line k and the emergency rating of the line. The expression for the continuous severity in the line k is defined as done by McCalley et al. (2003). Continuous severity functions, if compared to discrete severity functions, have the advantage of providing non zero risk results for scenarios close to the performance limits, but not failure, which reflect the realistic sense that a near violation scenario is as a matter of facts risky. Mathematical formulation can be expressed as follows:

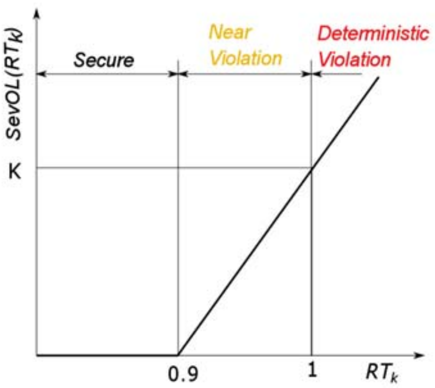

Fig. 1. Example of Severity function for line over load. Secure flow levels, near violation and deterministic violation flow levels are presented.

$$SevOL_k(PR_k) = \begin{cases} d * PR_k + c & \text{if } PR_k \geq PR_k^{min} \\ 0, & \text{otherwise} \end{cases} \tag{3}$$

The deterministic limit for violation is PR_k=1, the near violation region is PR_k $\leq$0.9, the value PR_k under 0.9 is regarded as safe, PR_k^{min}=0.9, *d*=10 and *c*=-9. Figure 1 is an illustrative example of continuous over-load severity function, secure near violation and deterministic violations levels are displayed.

2.3. *Cascading index*

Generally speaking, a "cascading" is a sequential successions of dependent events. In power system cascading analysis, many are the factors that can contributed or generate a sequence of undesired events. In a general way, line tripping can have two origins, one is load-driven when thermal expansion can result in the line dropping beneath its safety clearance, and one is load-independent, i.e. mechanical failure. In the adopted model, overload events are the one accounted for, the metric adopted to assess the cascading overload risk is analogous to the one presented in J. McCalley et al.(2003):

$$CEI(\zeta) = \sum_{i=1}^{N_c} \sum_{k=1}^{N_l} \mathcal{P}(C_k|C_i, \zeta) SevOL_k(C_i, \zeta) \tag{4}$$

where $\mathcal{P}(C_k|C_i)$ is the probability of secondary trip of line k after the failure of line i. The probability of cascading trip of line k after a initiating contingency i can be expressed as follows:

$$\mathcal{P}(C_j|C_i) = \begin{cases} \dfrac{P_j(C_i,\zeta) - P_{0,j}(\zeta)}{P_{trip,j}(C_i,\zeta) - P_{0,j}(\zeta)} & \text{if } P_j(C_i,\zeta) \geq 0.9P_{emerg,j} \\ 0, & \text{otherwise} \end{cases} \tag{5}$$

where $P_j(C_i, \zeta)$ is the post-contingency flow on circuit j given contingency i and condition ζ, $P_{trip,j}(C_i, \zeta)$ is defined as the flow leading to a certain trip of the line j (assumed to be 125% of its maximum capacity) and $P_{0,j}(\zeta)$ is the pre-contingency flow in the line j if condition ζ holds. Equation 5 is related to the fact that higher load levels and larger transients increases the likelihood of cascading event on circuit k after initiating event on circuit i.

3. Uncertainty Modelling

Adequately model uncertainty is paramount to improve robustness of the analysis accounting both lack of information and randomness of processes which are by their nature stochastic (e.g. environmental conditions, future power demand, power produced by RES, etc.). Generally speaking, uncertainty can be separated in two groups, the so called aleatory and epistemic uncertainties, as explained in A. Der et al. (2009) or R. Rocchetta, M. Broggi and E. Patelli (2015). The aleatory is related to stochastic behaviours and randomness in events and variables. The epistemic is commonly related to lack of knowledge about a particular behaviour, imprecision in measurement and poorly designed models. In this work, aleatory uncertainties related to the stochastic weather conditions and operational conditions are accounted for. In this stage of the work the framework do not include any sources of epistemic uncertainty which have been therefore neglected.

3.1. *Weather Modelling*

Markovian models for wind speed have been proposed in the literature, examples are A. D. Sahin et al. (2001) and A. Shamshad (2005). Markov process have been successfully applied by H. Morf (2014) in modelling the randomness of cloud covered solar irradiation. In the proposed model, the thickness of the clouds affects the intensity of sunlight and, hence, the amount of energy per unit of time produced by the solar cell. Similarly, the wind speed influence the power produced by the wind turbines distributed over the grid. The evolution of the wind speed and sun radiation process can be expressed, e.g. for the wind, by using the stochastic matrix of state changes defined as follows:

$$\mathbf{p_{t,t+1}}_v = \begin{bmatrix} p_{1,1} & p_{1,2} & \cdots & p_{1,n} \\ p_{2,1} & p_{2,2} & \cdots & p_{2,n} \\ \vdots & \vdots & \ddots & \vdots \\ p_{n,1} & p_{n,2} & \cdots & p_{n,n} \end{bmatrix}_v \tag{6}$$

where $p_{i,j}$ represent the probability of transition from state i at the hour t to state j at the hour $t+1$ and the subscript v refers to the quantity wind speed. Each entry of in the transition matrix have to satisfy the non-negativity $p_{i,j} \geq 0$ and normalization conditions $\sum_{j=1}^{n} p_{i,j} = 1$.

$$\mathbf{S_v} = \begin{bmatrix} S_0 \ S_2 \ldots S_n \end{bmatrix}_v \tag{7}$$

where S_j is the j^{th} state of the environmental variable of interest. In practice, the transition probability matrix elements constitute i.e. the relative frequency of the measured wind speeds that fall into the j^{th} state at time $t+1$ provided that it was at the i^{th} state at the previous time step.

3.2. *Load Demand Model*

The aggregated load connected to a node can be described by a Normal distribution R. Mena et al. (2014). Its corresponding PDF is the following:

$$f(P_{L,i}(t)) = \frac{1}{\sqrt{(2\pi)\sigma_i(t)}} exp\left(-\frac{(P_{L,i}(t) - \mu_i(t))}{2\sigma_i(t)^2}\right) \tag{8}$$

where $P_{L,i}(t)$ is the load demand or power withdrawn form node i at hour of the day t, μ_i is the load mean value and σ_i is the standard deviation at node i and time t. The parameter of the distribution can be estimated from historical records of load demand per node and hour.

4. Main Power Generators and DGs Modelling

Main power Generators (MG) are traditional large size generators often located far from the power demand and final users. Assigned minimum, maximum power outputs and power production costs per generator, the power produced by the main generators is determined by an optimal power dispatch problem summarized in Section 5. DGs considered in this framework are wind turbines, photovoltaic generators and electric vehicles. The power generation model for the technologies are in line with previous studies proposed by Y.-F. Li and E. Zio (2012).

The WT produces power by transforming the kinetic energy of the wind to electric energy. The power output of one turbine can be determined through relation with the wind speed intensity as follows:

$$P_w(v(t)) = \begin{cases} P_w^{rated} \dfrac{v(t) - v_{ci}}{v_r - v_{ci}} & \text{if } v_{ci} \geq v(t) < v_r \\ P_w^{rated} & \text{if } v_r \geq v(t) < v_{co} \\ 0, & \text{otherwise} \end{cases} \tag{9}$$

where v_{ci} is the cut-in wind speed [m/s], v_r is the rated wind speed [m/s], v_{co} is the cut-out wind speed [m/s] and P_w^{rated} is the rated power [kW].

The power output from a PV cell can be obtained using the relation with simulated irradiation s(t) and other parameters as in R. Mena et al. (2014):

$$P_{pv}(s(t)) = n_{cells} * FF * V * I \tag{10}$$

where FF fill factor, n_{cells} number of photovoltaic cells, P_{pv} (s) PV power output [W] and V and I are voltage and current of the PV cell.

4.1. *Electric Vehicles model*

Generally speaking, three possible operating states (*op*) can be accounted, the Grid to Vehicle (e.g. Charging battery), Vehicle to Grid (e.g. Discharging battery) and the disconnected operative states. In this work, these three operating conditions have been included in the probabilistic framework accounting three strategies, first strategy is named ”no-V2G strategy”, the second and third are named “V2G strategy1” and “V2G strategy 2”. Different probability

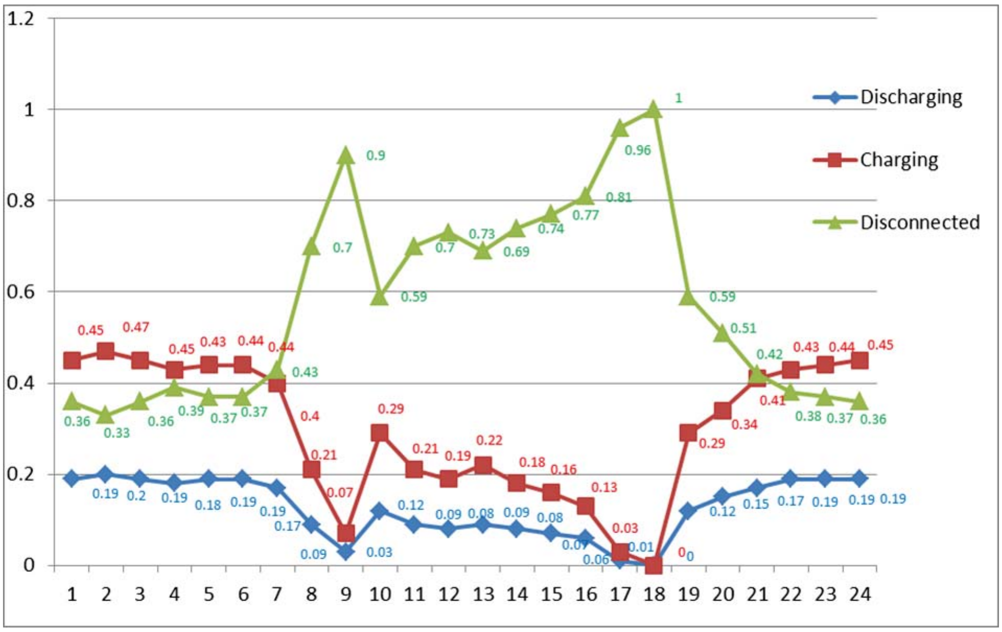

Fig. 2. $f(t, op)$ and probability masses for three *op*conditions,V2G strategy 1.

masses have been associated to different *op* and strategies. Figure 2 display probability masses for V2G strategy 1. Power outputs of one EVs, $f(t, op)$ are calculated as proposed by Y. Li and E. Zio (2012):

$$f(t, op) = \begin{cases} p_{V2G}(t) \text{ if } op = V2G \\ p_{G2V}(t) \text{ if } op = G2V \\ p_{disconnected}(t) \text{ if } op = discon. \end{cases} \tag{11}$$

where $p_{V2G}(t)$ is the V2G operative state probability at time t, $p_{G2V}(t)$ is the G2V operative state probability at time t, $p_{discon.}(t)$ is the probability of EV disconnected at time t and *op* is the EV operative state.

5. DC Optimal Power Flow

Direct current (DC) power flow is a variations of the Newton method which account for just active power, neglecting power loses, voltage support and reactive power management. It is often presented to alleviate the computational time demanded by some analysis (e.g. robust optimization) and it is usually adopted in transmission network analysis, see as example K. Purchala et al. (2005), but can be found also in distribution systems analysis.

Under the DC power flow assumptions, the nodal power equations and can be rewritten as in equations 12-13:

$$P_i = \sum_{j=1}^{N_n} B_{i,j} \left(\delta_i - \delta_j \right) \tag{12}$$

$$\sum_i (P_{w,i} + P_{pv,i} + P_{ev,i} + P_{MG,i} - P_{L,i} - P_i) = 0 \tag{13}$$

where P_i is the active power flowing from the node i to the network [kW], $B_{i,j}$ is the susceptance of the line connecting node i to node j in [$\frac{1}{\Omega}$], δ_i is the voltage angle of node i and N_n is the total number of nodes in the system. $P_{w,i}$, $P_{pv,i}$, and $P_{ev,i}$ are the power produced or demanded (e.g. Electric vehicles) by the DGs, $P_{MG,i}$ is the power produced by the main generator $P_{L,i}$ is the power load demand in the node i. Equations 12-13 hold for each node in the network. The DC power flow can be usefully embedded to economical minimization problem to find the best power scheduling in order to minimize a cost function.

$$min\ C_{op} \left(\mathbf{P}_{G,i}, ep \right) \tag{14}$$

The DC optimal power flow (DC-OPF) refer to this type of optimization as summarized in equation 14, which is subject to equity constraints, e.g. equations 12-13 and inequality constraints, minimum and maximum power outputs and maximum line capacities.

The term C_{op} is the network operative cost,$\mathbf{P}_{G,i}$ represent the power injection in node i,$\mathbf{P}_{G,i} = [P_w, P_{pv}, P_{ev}, P_{MG}]_i$ and *ep* is the estimated electricity price for a given load demand, as in Mena et al. (2015). It worth remark that the operative cost of the network is dependent on the power generation and supply which are direct output of the DC-OPF.

6. Numerical implementation

This section presents the numerical implementation of the proposed computational strategy, proposed to speed up the analysis. Procedure for the simulations is as follows:

- Step1: Netwrok Data, generator data, RES data, weather data are loaded.
- Step2: Set number of hours for a simulation T_h, generate $s(t)$, $v(t)$ and $P_{L,i}$ $\forall$ node i and $t = 1, 2, .., T_h$ as presented in section 3.
- Step3: For each strategy (no V2G, V2G strategy 1, V2G strategy 2) and for $t = 1, 2, .., T_h$ perform risk assessment as in algorithm 1;
- Step4: Expected $E(R(\zeta))$, $E(CEI(\zeta))$ and $E(C_{op})$ along the simulated hours are obtained and contingency ranking performed;
- Step5: Different strategies are compared.

Algorithm 1 Risk Assessment for a simulated hour

procedure CASCADING AND OVER LOAD RISK ASSESSMENT
    Randomize *op* $\forall$ node.
    Compute: $P_{ev,i}(t, op)$, $P_{w,i}(v(t))$, $P_{pv,i}(s(t))$ $\forall i$
    Solve: pre-contingency DC-OPF
    Save: $P_{0,k}(\zeta)$ $\forall$ line k, minimum C_{op}
    for $i = 1$ to N_c **do**
        Solve DC-OPF for contingency state C_i
        $P_k(C_i|\zeta)$ $\forall$ line k
        for $k = 1$ to N_l **do**
            Compute: $\mathcal{P}(C_k|C_i, \zeta)$ and $SevOL_k(C_i, \zeta)$ as in Equations 5and 3
        end for
        Compute: $\mathcal{P}(C_i|\zeta)$ as in Equations 2
        $R(C_i|\zeta) = \sum_{k=1}^{N_l} \mathcal{P}(C_i|\zeta) SevOL_k(C_i, \zeta)$
    end for
    Compute: cascading index and over-load Risk:
    $CEI(\zeta) = \sum_{i=1}^{N_c} \sum_{k=1}^{N_l} \mathcal{P}(C_k|C_i, \zeta) SevOL_k(C_i, \zeta)$
    $R(\zeta) = \sum_{i=1}^{N_c} R(C_i|\zeta)$
end procedure

In order to reduce the computational effort, DC-OPF for contingency states have been performed in parallel on a computed cluster.

7. Case Study

In this work an adapted version of the IEEE 24 nodes reliability test system has been adopted to test the goodness of the framework in providing risk assessment of different EVs control strategies. The original network count 24 nodes, 7 main generating units and 34 lines which makes it relatively complex and suitable for the analysis. In order to better cope with the aim of the work some modification has been implemented to the original system as described in the following subsections.

7.1. *The Modified IEEE 24 bus test system*

Figure 3 shows original interconnection between nodes and original main generating units position. The original system include 12 main generators allocated on 10 different nodes. The

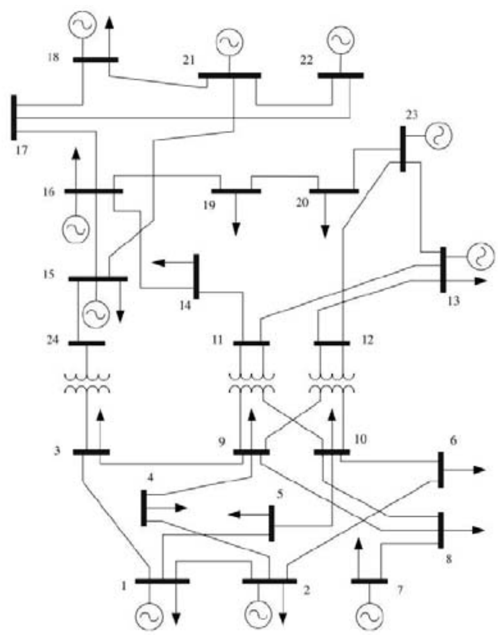

Fig. 3. The IEEE 24 nodes reliability test system

technical characteristics of the feeders, i.e. estimated λ_k, $B_{i,j}$, l_k, maximum capacity, the technical data of the main generating units, minimum and maximum power outputs and costs and load data, are findable in the technical report of P. Wong et al. (1999), the IEEE reliability test system. In the modified version, the following changes have been implemented:

- Connection line between node 5 and node 7 has been added. Line characteristic are equivalent to the one of line connecting node 5 to node 10;
- Load demand has been incremented of 25%;

- WT and PV generators have been allocated in each node of the grid to reach the 15% and 5% of penetration respectively;
- EVs have been allocated in the gird nodes, uniform 5% penetration level has been accounted;

Modifications are made in order to avoid islanding scenarios(e.g. line between node 7 and 8 fails) and to justify allocations of DGs (e.g. increment in the load demand). In line with the work proposed by R. Rocchetta, Y. Li, E. Zio (2015), the selected contingency list include just the 'N-1' line contingencies, therefore N_c is set equal to 35 (the number of lines in the modified system). A series of published papers have proposed 'N-1-1' or 'N-k' contingency analysis , as example G. Chen et al. (2015) or D. Chatterjee et al. (2010), but analyse a comprehensive list of contingencies has been considered out from the final scope of the work.

Photovoltaic generators and wind turbines technical parameters are findable in Mena et al. (2014). Power demand have been assumed normal distributed around the mean value with standard deviation equal to the 5% of the mean value

.

7.2. *Weather Data*

Wind speed and sun irradiation at the simulated hour 1 are randomly selected between the possible wind speed and solar radiation states, wile for the following simulated hours the weather conditions are obtained as explained in section 3. The framework is flexible enough to account different environmental conditions in different nodes, however wind speed and sun radiance have been assumed to be constant for a given time on the network. An illustrative example of the generated wind speed data is presented in figure 4. The plots show in the x-axis one year of simulated hours and in y axis $v(t)$.

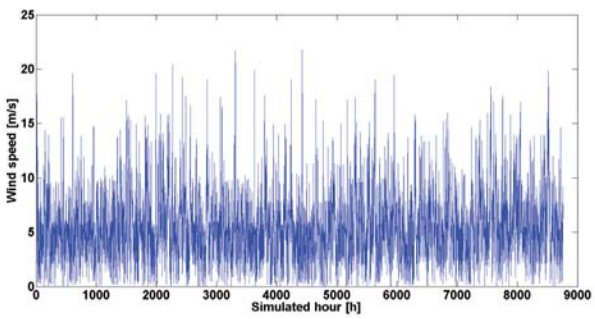

Fig. 4. One Year Simulated v

For the data on transition matrix for wind speed states and sun radiance states, the reader is reminded to references A. Shamshad et al. (2005) and H. Morf (2014) respectively. The simulated $s(t)$ refers to a location with latitude 45 ° and longitude -8 °.

7.3. *EV strategy data*

Three different strategies have been analysed as mentioned in subsection 4.1. The probabilities $p_{V2G}(t)$, $p_{G2V}(t)$ and $p_{disconnected}(t)$ for "V2G strategy 1" are displayed in figure 2, "no V2G" strategy is equal to "V2G strategy 1", but if a V2G operative state is randomized, the vehicle is assumed as disconnected. Probability masses for V2G strategy 2 are displayed in figure 5.

It can be noticed that V2G strategy 1 and V2G strategy 2 differs due to different probability masses associated to different operational states and hours.

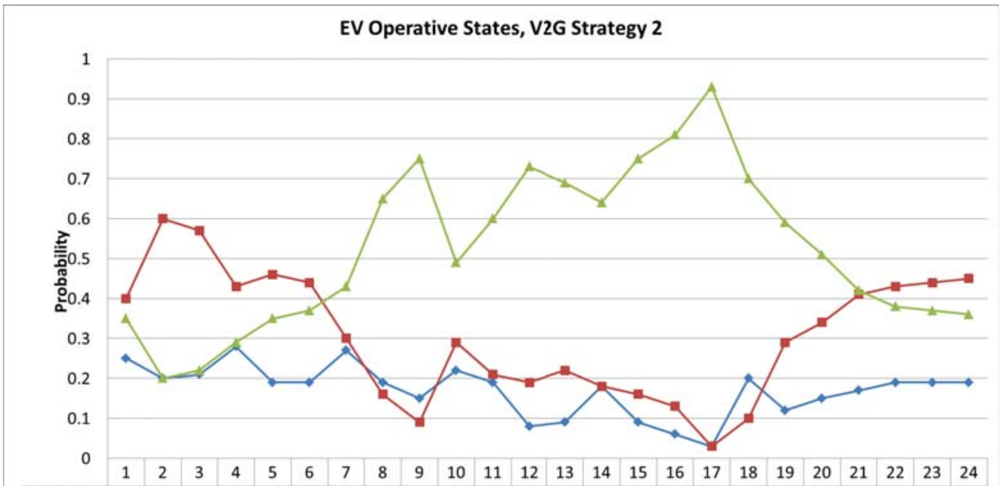

	1	2	3	4	5	6	7	8	9	10	11	12	13	14	15	16	17	18	19	20	21	22	23	24
V2G	0.25	0.2	0.21	0.28	0.19	0.19	0.27	0.19	0.15	0.22	0.19	0.08	0.09	0.18	0.09	0.06	0.03	0.2	0.12	0.15	0.17	0.19	0.19	0.19
G2V	0.4	0.6	0.57	0.43	0.46	0.44	0.3	0.16	0.09	0.29	0.21	0.19	0.22	0.18	0.16	0.13	0.03	0.1	0.29	0.34	0.41	0.43	0.44	0.45
Discon.	0.35	0.2	0.22	0.29	0.35	0.37	0.43	0.65	0.75	0.49	0.6	0.73	0.69	0.64	0.75	0.81	0.93	0.7	0.59	0.51	0.42	0.38	0.37	0.36

Fig. 5. $f(t, op)$ and probability masses for three *op* conditions, V2G strategy 2.

8. Results

The computational framework described allows risk visualization and contribution to overall risk due to the different contingencies, risk assessment and comparison of different EVs control strategies and hourly and global contingency ranking.

8.1. *EV Strategies Risk and Cost Comparison*

Expected cascading index $E(CEI)$ for the three considered strategies have been plotted along the simulated hours as displayed in figure 6, for synthesis expected $R(\zeta)$ and C_{op} are not displayed. The no V2G strategy results as the more risky and more expensive than V2G strategies 1 and 2.

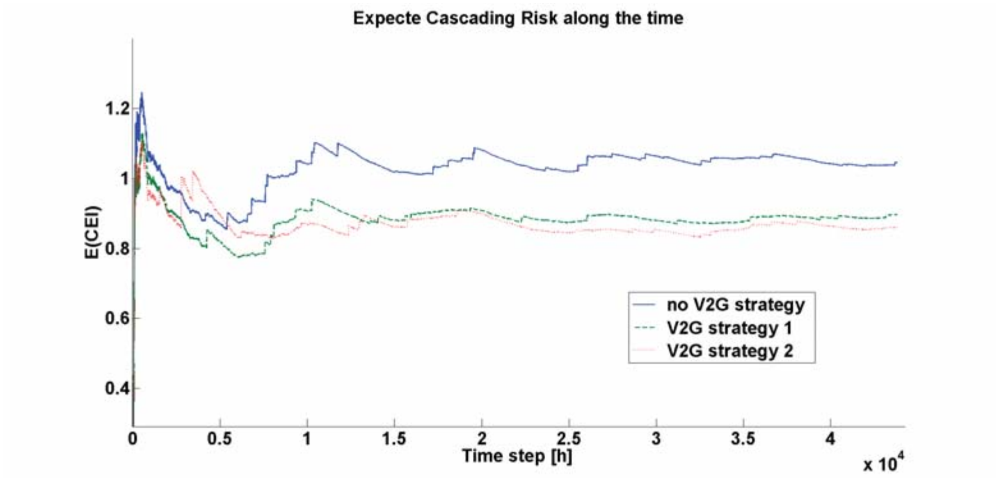

Fig. 6. Expected CEI index for three strategies along with the simulated hours.

Results show that V2G strategy 2 perform better than all the others strategies reducing both cascading and overload risks, this is explainable within the model because strategy 2 have higher probability of result in a V2G states in the central hour of the day (when load demand is higher), hence producing a positive increase in the nodal energy self-consumption hence reducing the lines stress and overall risk.

8.2. *Contingency Ranking*

Figure 7 shows the overall contingency ranking as expected value of the ratio $\frac{R(C_i|\zeta)}{R(\zeta)}$. It can be seen that failure of the line between node 15 and 21 contribute the most to the overload risk with approximatively 76%, 70% and 72% for the no-V2G strategy, V2G strategy 1 and V2G strategy 2 respectively. Second and third higher contributions to the overload risk are due to line failure between nodes 2 and 6, with about 5.5%, 6.99% and 7.52% for no V2G strategy, V2G strategy 1 and V2G strategy 2 respectively and to line failure between nodes 20 and 23, about 4.6% 5.3% 5.8% respectively. Other contingencies contribute less to the total risk and some have almost null contribution. The two strategies that allow V2G operative mode, compared to the no-V2G one, have as effect a distribution of the risk between the contingencies, reducing the relevance of the most severe accident (e.g. C_{26} in figure 7), but increasing the contribution to the total risk of the less severe(e.g. C_5 or C_{34} in figure 7).

9. Remark and Discussions

In this paper an useful framework for simulation-based probabilistic risk assessment electric vehicles control strategies with renewable energy sources is presented. Uncertainty in the operative condition of the network and renewable power production have been included in the framework. Application to a case study shows that this framework is can be used in to

Ranking.png

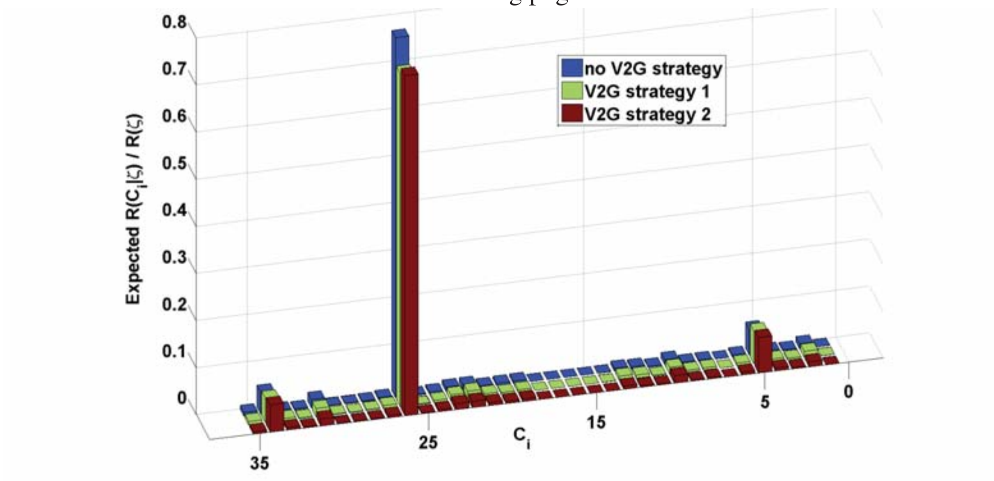

Fig. 7. Expected contingency ranking

assess risk of over load and cascading sequences if different electric vehicles control strategies are adopted. Expected contingency ranking has been originally performed and ranks under different strategies have been compared and discussed.

References

[1] A. D. Sahin, Z. Sen, First-order markov chain approach to wind speed modelling, Journal of Wind Engineering and Industrial Aerodynamics 89 (3?4) (2001) 263 – 269, 10th International Conference on Wind Engineering.

[2] A. Der Kiureghian, O. Ditlevsen, Aleatory or epistemic? does it matter?, Structural Safety 31 (2) (2009) 105–112.

[3] A. Kavousi-Fard, A. Abunasri, A. Zare, R. Hoseinzadeh, Impact of plug-in hybrid electric vehicles charging demand on the optimal energy management of renewable micro-grids, Energy 78 (2014) 904 – 915.

[4] A. Shamshad, M. Bawadi, W. W. Hussin, T. Majid, S. Sanusi, First and second order markov chain models for synthetic generation of wind speed time series, Energy 30 (5) (2005) 693 – 708.

[5] D. Chatterjee, J. Webb, Q. Gao, M. Vaiman, M. Vaiman, M. Povolotskiy, N-1-1 ac contingency analysis as a part of nerc compliance studies at midwest iso, in: Transmission and Distribution Conference and Exposition, 2010 IEEE PES, 2010, pp. 1–7.

[6] F. Xiao, J. McCalley, Power system risk assessment and control in a multiobjective framework, Power Systems, IEEE Transactions on 24 (1) (2009) 78–85.

[7] G. Chen, Y. Dai, Z. Xu, Z. Dong, Y. Xue, A flexible framework of line power flow

estimation for high-order contingency analysis, International Journal of Electrical Power & Energy Systems 70 (2015) 1 – 8.

[8] H. Falaghi, C. Singh, M.-R. Haghifam, M. Ramezani, {DG} integrated multistage distribution system expansion planning, International Journal of Electrical Power & Energy Systems 33 (8) (2011) 1489 – 1497.

[9] H. Hashemi-Dezaki, M. Hamzeh, H. Askarian-Abyaneh, H. Haeri-Khiavi, Risk management of smart grids based on managed charging of phevs and vehicle-to-grid strategy using monte carlo simulation, Energy Conversion and Management 100 (2015) 262–276.

[10] H. Morf, Sunshine and cloud cover prediction based on markov processes, Solar Energy 110 (2014) 615 – 626.

[11] J. McCalley, F. Xiao, Y. Jiang, Q. Chen, Computation of contingency probabilities for electric transmission decision problems, in: Intelligent Systems Application to Power Systems, 2005. Proceedings of the 13th International Conference on, 2005, pp. 540–545.

[12] J. McCalley, M. Ni, V. Vittal, T. Tayyib, Online risk-based security assessment, IEEE Transactions on Power Systems 18 (1) (2003) 258–265.

[13] J. McCalley, S. Asgarpoor, L. Bertling, R. Billinion, H. Chao, J. Chen, J. Endrenyi, R. Fletcher, A. Ford, C. Grigg, G. Hamoud, D. Logan, A. Meliopoulos, M. Ni, N. Rau, L. Salvaderi, M. Schilling, Y. Schlumberger, A. Schneider, C. Singh, Probabilistic security assessment for power system operations, in: Power Engineering Society General Meeting, 2004. IEEE, 2004, pp. 212–220 Vol.1.

[14] K. Purchala, L. Meeus, D. Van Dommelen, R. Belmans, Usefulness of DC power flow for active power flow analysis, in: Power Engineering Society General Meeting, 2005. IEEE, 2005, pp. 454–459 Vol. 1.

[15] M. Čepin, Analysis of truncation limit in probabilistic safety assessment, Reliability Engineering & System Safety 87 (3) (2005) 395 – 403.

[16] M. van der Kam, W. van Sark, Smart charging of electric vehicles with photovoltaic power and vehicle-to-grid technology in a microgrid; a case study, Applied Energy 152 (2015) 20 – 30.

[17] M. Yilmaz, P. Krein, Review of benefits and challenges of vehicle-to-grid technology, in: Energy Conversion Congress and Exposition (ECCE), 2012 IEEE, 2012, pp. 3082–3089.

[18] L. Liu, F. Kong, X. Liu, Y. Peng, Q. Wang, A review on electric vehicles interacting with renewable energy in smart grid, Renewable and Sustainable Energy Reviews 51 (2015) 648 – 661.

[19] R. Brown, Electric Power Distribution Reliability, Power Engineering (Willis), CRC Press, 2002.

[20] R. Rocchetta, Y. Li, E. Zio, Risk assessment and risk-cost optimization of distributed

power generation systems considering extreme weather conditions, Reliability Engineering & System Safety 136 (0) (2015) 47 – 61.

[21] R. Rocchetta, M. Broggi, E. Patelli, Efficent epistemic-aleatory uncertainty quantification: Application to the nafems challenge problem, in: NAFEMS World Congress 2015, At San Diego, CA, 2015.

[22] R. Mena, M. Hennebel, Y.-F. Li, C. Ruiz, E. Zio, A risk-based simulation and multi-objective optimization framework for the integration of distributed renewable generation and storage, Renewable and Sustainable Energy Reviews 37 (2014) 778 – 793.

[23] P. Wong, P. Albrecht, R. Allan, R. Billinton, Q. Chen, C. Fong, S. Haddad, W. Li, R. Mukerji, D. Patton, A. Schneider, M. Shahidehpour, C. Singh, The ieee reliability test system-1996. a report prepared by the reliability test system task force of the application of probability methods subcommittee, Power Systems, IEEE Transactions on 14 (3) (1999) 1010–1020.

[24] Y. Li, E. Zio, Uncertainty analysis of the adequacy assessment model of a distributed generation system, Renewable Energy 41 (2012) 235 – 244.

[25] Z. Liu, D. Wang, H. Jia, N. Djilali, Power system operation risk analysis considering charging load self-management of plug-in hybrid electric vehicles, Applied Energy 136 (2014) 662 – 670.